IEEE Access
Multidisciplinary ⋮ Rapid Review ⋮ Open Access Journal

Received 12 June 2024, accepted 22 June 2024, date of publication 26 June 2024, date of current version 5 July 2024.

Digital Object Identifier 10.1109/ACCESS.2024.3419226

RESEARCH ARTICLE

Co-Optimization Strategy of Island Distribution Grid and Time-of-Use Pricing Considering the Time Response Characteristics of Multiple Interruptible Loads

WEIJIE HE[1], LANXUAN GUO[1], WENHAO YANG[1], XIANGNING LIN[1], (Senior Member, IEEE), FANRONG WEI[1], AND SAMIR M. DAWOUD[2]

[1]State Key Laboratory of Advanced Electromagnetic Engineering and Technology, Huazhong University of Science and Technology, Wuhan, Hubei 430074, China

[2]Department of Electrical Power and Machines Engineering, Faculty of Engineering, Tanta University, Tanta 31527, Egypt

Corresponding author: Lanxuan Guo (1354460578@qq.com)

This work was supported in part by the National Key Research and Development Program of China under Grant 2022YFE0120400, and in part by the National Natural Science Foundation of China under Grant U22B20106.

ABSTRACT Currently, island grids are being rapidly constructed in various regions, and the stochastic nature of renewable energy generation output provides a great challenge for the economic dispatch of island grids. In terms of demand-side management, the models used in existing studies in considering time-of-use pricing as well as interruptible loads are still relatively simple, which makes it difficult to fully utilize their potentials in scenarios where the number and types of controllable loads in the distribution network are increasing. For this reason, this paper firstly analyzes the time response characteristics of users participating in interruptible load protocols. Moreover, this paper proposes corresponding time-domain compensation means, and establishes a multi-type active load model based on time-of-use pricing. Secondly, the time-of-use pricing setting and the optimal scheduling of the active distribution network are integrated into a unified optimization problem in order to strengthen the guiding effect of the time-of-use pricing mechanism on the users and to achieve the overall economic optimization. Finally, a mixed integer nonlinear programming model for day-ahead and intraday integrated scheduling is developed to consider the source-storage-load characteristics within the distribution grid. Compared with the constant tariff model and the traditional TOU model, the co-optimization method of time-of-use pricing formulation and active distribution grid dispatch are improved in terms of economic efficiency of the island grid.

INDEX TERMS Island distribution networks, renewable energy generation, time-of-use pricing, ILs, grid scheduling.

I. INTRODUCTION

The development of a low-carbon, green and ecologically friendly island energy resource security system has become a common demand for global energy system change [1], and it is of great significance for increasing the proportion of renewable energy, promoting the clean and efficient use of energy, and enhancing the efficiency of comprehensive energy utilization. However, the coupling and coexistence of multiple energy chains, the diversification of energy-use scenarios, the large differences in resource endowments, and the cooperation and competition among energy trading entities have made the optimization of energy supply and operation of islands face great challenges [2]. On the one hand, this enriches the control means and operation mode of the power grid, but at the same time, it also makes the operation and control of the distribution network more complex [3], and the control strategy and operation mode of the traditional

The associate editor coordinating the review of this manuscript and approving it for publication was Fabio Mottola.

distribution network need to be expanded. Therefore, it is necessary to propose operation and control strategies that can coordinate distributed generation, controllable loads and energy storage.

At present, the research on the modeling and application problems of distributed generation and energy storage in distribution networks has been relatively mature [4]. Distribution grid scheduling and operation based on demand side response (DSR) has also become more and more a hot research topic in academia [5]. However, in terms of demand side management (DSM), the existing research mainly focuses on time-of-use pricing (TOU) [6] and traditional interruptible loads (IL). But the models used are still relatively sketchy and one-sided [7], which makes it difficult to fully utilize its potential.

In terms of real-time electricity prices, since electricity providers and users are not a unified whole, in order to balance the interests of all parties, scholars have begun to study the real-time electricity price problem from the perspective of the game. The study [8] proposed a new pricing structure, named as a real-time variable peak pricing scheme with a self-inbuilt feature to capture the benefit of both the existing pricing scheme. Although the privacy and comfort of users are taken care of in the system modeling, benefits to electricity suppliers are not included in the game model. At present, in order to reduce the volatility of renewable energy access, today's scholars have begun to improve the real-time electricity price model. In [9], the incentive mechanisms were designed to increase the flexibility of distributed energy systems, and it proposed a virtual real-time tariff optimization model based on credit mechanisms, which lacked consideration of overall economics. The study in [10] proposed an inter-provincial two-tier market clearing decision model, where the upper tier optimizes the provincial market through a unilateral bidding model, and the lower tier optimizes power purchases by minimizing the cost of acquiring inter-provincial renewable energy. Despite the improved operational economics of the distribution network under this strategy, the impact of demand-side response was still ignored. In [11], a fair pricing scheme based on power demand forecasting was proposed to reduce extra bills of low energy consumers. In addition, the program did effectively incentivize low energy consumers, but the utility did not reap the benefits of the strategy. With the development of artificial intelligence algorithms, neural networks have also been widely used in electricity price prediction. The research in [12] proved that convolutional neural network with long and short-term memory network better handles the sinusoidal characteristics and volatility of electricity price compared to multiple linear regression model and predicts the daily voltages in Iranian energy market well. And in [13], an advanced deep neural network with long and short term memory combined with feature selection algorithm was applied for electricity price prediction. The results from the proposed model in an empirical study of the Nordic market were precise. However, each of the above strategies focuses on the price mechanism itself, and the pricing optimization is cut off from the economic dispatch of the distribution network, which prevents the optimal solution from being obtained.

Moreover, current IL protocols are mainly deterministic, and they can only be used by specific types of industrial users [14] and do not fully utilize the regulatory potential of different types of users. As a matter of fact, IL resources are becoming more and more available in island distribution networks with the wide distribution of energy storage and the increased controllability of electricity consumption by users. The study in [15] pointed out that the extensive contracting of IL with multiple types of users is effective in reducing peak loads and operating prices in future smart cities. To better manage IL, studies in both [16] and [17] have developed smart energy management system and user behavior models for DSM, respectively. A source-load-storage multiple standby capacity system was constructed in [18] for IL-containing gas and electricity systems, which could realize the coordinated operation of multiple resources and adequately cope with load-side and source-side output fluctuations. The downside is that the study lacked the construction of specific response model of IL. The study in [19] established a bi-level capacity optimization model that considered load demand management. By controlling the interruptible and shiftable loads, the model could optimize load characteristics, reduce operation costs, and increase system stability. But it ignored the impact of TOU on loads. In summary, these models only considered detailed user response models to the excitation, and rarely took into account the response time characteristics of the users.

Therefore, in order to improve the operational economic efficiency of the island distribution network after renewable energy generation access, this study establishes a synergistic optimization model of TOU and distribution network operation with the participation of multiple types of controllable loads, and mainly carries out the following work:

First, we analyze response time characteristics of the users participating in the IL protocol, propose the corresponding time-domain compensation means, and establish a multi-type active load model based on the TOU;

Second, TOU setting and optimal scheduling of the island distribution network are integrated into a unified optimization problem in order to enhance the guiding effect of the TOU mechanism on the users and to achieve the overall economic optimality;

Third, we develop a mixed-integer nonlinear model considering the source-storage-load characteristics within the active island distribution network for day-ahead and intraday integrated scheduling, which maximizes the overall economic benefits of the user side and the grid side.

II. ISLAND SOURCE-STORAGE-LOAD MODEL

In order to maintain the stability of power supply, renewable energy generation units, energy storage, micro fuel engine and active loads are used as the main control objects for the operation of the island distribution network, and the basic

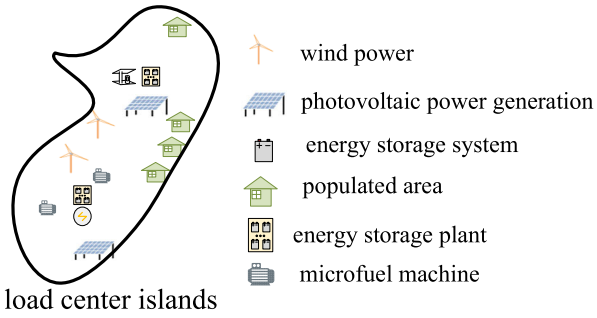

FIGURE 1. Island distribution network structure.

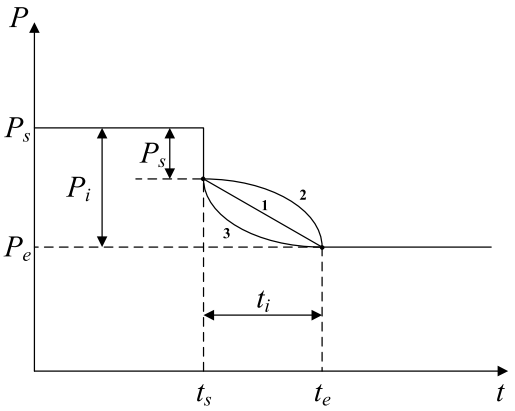

FIGURE 2. IL time response characteristics.

model of the island distribution network is shown in Figure 1. Its cost and operation model is an important part of the distribution network source-storage-load coordinated control strategy, which is briefly described below respectively.

A. ACTIVE LOAD MODEL

1) MODELING OF CUSTOMER RESPONSE TO REAL-TIME ELECTRICITY PRICES

For all users as a whole, their electricity price response behavior is modeled based on the price elasticity coefficient. Load users respond to the current period's tariff change and actively cut down when the tariff is higher, which is manifested as the self-elasticity coefficient, while the leveling load users will choose the optimal time to use electricity based on the comparison of tariffs in multiple time periods, i.e., the load in the current period will also be affected by the tariffs of other time periods, which is manifested as the mutual elasticity coefficient, which is shown in equation (1) and equation (2):

$$\varepsilon_{ii} = \frac{\Delta d_i/d_i}{\Delta p_i/p_i} \tag{1}$$

$$\varepsilon_{ij} = \frac{\Delta d_i/d_i}{\Delta p_j/p_j} \tag{2}$$

where, ε_{ii} is the auto-elasticity coefficient of time period i, ε_{ij} is the mutual elasticity coefficient of time period i to time period j, Δd_i denotes the change in quantity demanded in time period I, d_i denotes the initial quantity demanded in time period i, Δp_i and Δp_j denotes the change in price in time period i and time period j, respectively, p_i and p_j denotes the initial price in time period i and time period j, respectively.

Based on the above definition of self-elasticity coefficient and mutual elasticity coefficient, the change of load quantity and the change of price for n periods in a day should be satisfied:

$$\Delta\mathbf{d} = \mathbf{E}\Delta\mathbf{p} \tag{3}$$

$$\Delta\mathbf{d} = [\Delta d_1/d_1, \Delta d_2/d_2, \ldots, \Delta d_n/d_n]^T \tag{4}$$

$$\Delta\mathbf{p} = [\Delta p_1/p_1, \Delta p_2/p_2, \ldots, \Delta p_n/p_n]^T \tag{5}$$

$$\mathbf{E} = \begin{bmatrix} \varepsilon_{11} & \varepsilon_{12} & \cdots & \varepsilon_{1n} \\ \varepsilon_{21} & \varepsilon_{22} & \cdots & \varepsilon_{2n} \\ \vdots & \vdots & \ddots & \vdots \\ \varepsilon_{n1} & \varepsilon_{n2} & \cdots & \varepsilon_{nn} \end{bmatrix} \tag{6}$$

where $\Delta\mathbf{d}$ is the vector of demand changes, $\Delta\mathbf{p}$ is the vector of price changes, and $\mathbf{E}$ is the matrix of elasticity coefficients.

Based on equations (3)∼(6), the load access situation of each load node under TOU can be calculated based on the load forecast information of each load node. At present, the island power grid load nodes are few, the load capacity is small, the power grid can obtain real-time access to power users' electricity consumption, providing the necessary data base for the power grid to analyze the user's electricity consumption habits, and load forecasting based on the node as a unit is feasible in the island distribution network scheduling.

2) TIME RESPONSE CHARACTERISTICS OF IL

Large users, such as factories, and small users, such as commercial and residential clusters, can sign an agreement with the grid to curtail some of their loads when power supply is tight, and gain more revenue by supporting the safe operation of the grid. Traditionally, IL agreements are signed between the grid and large industrial or commercial users, but in island grids, the ease of measurement enables small users (e.g., residential users) to participate in demand-side response [20]. However, due to the diversity of cluster users, interruptible is usually in a different state when a command is issued, making it difficult to cut off all loads immediately. Therefore, response time modeling of interruptible loads is needed. This chapter assumes that the IL response characteristics are shown in Figure 2. After the grid issues an IL disconnection command at the time, the IL is disconnected instantly, and the remaining loads will be disconnected one after another during the time period due to the different states they are in, and will be completely disconnected at the time. In practice, the sensitivity of different user equipment to compensation is different. In order to reasonably consider the time response characteristics of IL, linear (curve 1), convex parabolic (curve 2) and concave parabolic (curve 3) models are constructed respectively.

As shown in Figure 2, immediate response α is defined as the ratio of the actual response P_s to the specified response P_i

at the moment of command, and response time t_i is defined as the time from the moment t_s of command to the moment t_e of full response:

$$\alpha = P_s/P_i \tag{7}$$

$$t_i = t_e - t_s \tag{8}$$

There are differences in the time response characteristics of different types of ILs, and describing them with all three models mentioned above will import some errors. However, in the control within the scheduling optimization step (15 min for intraday scheduling and 1 h for day-ahead scheduling), considering the need for IL convergence, the response is basically complete within one step and there is no need to model the process in a refined way.

In order to encourage users to disconnect loads in a timely manner at a given moment, the compensation cost of IL takes into account the amount and duration of interruptions, as well as the instantaneous responsiveness and response time. Based on the above considerations, the compensation factor for IL can be referred to equation (9):

$$\lambda = f(\alpha, t_i) = \alpha \cdot \lambda_0 + (1-\alpha) \cdot (1 - t_i/t_{i,0}) \cdot \lambda_0 \tag{9}$$

where, $t_{i,0}$ and λ_0 is the reference value of response time and compensation coefficient. Compensation coefficient is composed of two parts, instant response load is compensated according to the reference compensation coefficient, and delayed response load is compensated according to the length of response time, the longer the response time, the lower the compensation coefficient.

B. MICRO FUEL ENGINE COST AND OPERATION MODEL

Conventional micro fuel units are less efficient in generating electricity, and usually use combined cooling, heating and power (CCHP), taking into account the benefits of cooling and heating in their costs F^t_{MT}, which consist of start-up and shutdown losses, fuel consumption, pollutant emission control, and the benefits of CCHP:

$$\begin{aligned} F^t_{MT} = {} & (mo^t_{MG,on} \cdot d_{MG,on} + mo^t_{MG,off} \cdot d_{MG,off}) \\ & + u^t_{MG} \cdot f_{MG}(P^t_{MG} \cdot \Delta T) + u^t_{MG} \cdot g_{MG}(P^t_{MG} \cdot \Delta T) \\ & - u^t_{MG} \cdot b_{MG}(P^t_{MG} \cdot \Delta T) \end{aligned} \tag{10}$$

where, ΔT is the control step, $mo^t_{MG,on}$ and $mo^t_{MG,off}$ are the micro fuel engine start-stop state transition variables. $mo^t_{MG,on} = 1$ and $mo^t_{MG,off} = 1$ denote the start-up operation and the shutdown operation. $d_{MG,on}$ and $d_{MG,off}$ are the start-stop costs. u^t_{MG} denotes the micro fuel engine turbine start-stop state variable, with 1 denoting the start-up state and 0 denoting the shutdown state. P^t_{MG} denotes the output value of the time period of t, f_{MG} denotes the output cost of micro fuel engine, g_{MG} denotes the cost function of pollution control, b_{MG} denotes the benefit of heating and cooling. The operation constraints of the micro fuel engine mainly includes unit output limit constraints, unit creep rate constraints, unit minimum start/stop time constraints, and start/stop logic constraints.

Upper and lower limits of micro fuel output constraints:

Subject to micro fuel performance constraints, there are upper and lower limits on real-time unit output, as shown in equation (11):

$$0 \le P^t_{MG} \le P^{\max}_{MG} \tag{11}$$

where $P^{\max}_{MG}$ indicates the upper output limit of the micro fuel engine.

Micro fuel engine climb rate constraint:

The upward or downward creep rate limit for micro fuel engine power is shown in equation (12):

$$-R_d \cdot P^{\max}_{MG} \le P^t_{MG} - P^{t-1}_{MG} \le R_r \cdot P^{\max}_{MG} \tag{12}$$

where $P^{\max}_{MG}$ denotes the output value in time period t-1; R_r and R_d are the upward and downward creep rates of the micro-fired unit, respectively.

Minimum start-up and shutdown time for micro fuel engines:

Due to the requirements of the technical conditions of the micro fuel engine itself, the micro fuel engine start, must run for a period of time and can't be immediately shut down. Similarly, the micro fuel engine shutdown, must also be shut down for a period of time before running. Therefore, the minimum start-stop time constraint should be satisfied when developing the thermal unit generation plan, as shown in equation (13):

$$\begin{cases} (u^{t-1}_{MG} - u^t_{MG})(T_{t-1} - T^{on}) \ge 0 \\ (u^t_{MG} - u^{t-1}_{MG})(-T_{t-1} - T^{off}) \ge 0 \end{cases} \tag{13}$$

where, T_{t-1} is the time of startup/shutdown operation in time period t-1. If the micro fuel is on in time period t-1, it is positive, and vice versa is negative. If the micro fuel is on at time t-1, it is positive, and vice versa. T^{on} is the minimum running time of the micro fuel, and T^{off} is the minimum downtime of the micro fuel.

C. RENEWABLE ENERGY GENERATION COST AND OPERATION MODEL

The power of renewable energy generation is intermittent and fluctuating, such as wind power and photovoltaic power generation, which is related to the wind speed, the intensity of solar irradiation [21], and the characteristics of the generator. Therefore, the prediction of renewable energy power has been the basis for its effective utilization. For example, a number of models and algorithms have been used to predict wind power output on different time scales. Relevant commercial software can achieve high prediction accuracy in short-term and ultrashort-term wind power forecasting, e.g., short-term forecasting accuracy can reach 80% (root-mean-square error), and ultrashort-term forecasting accuracy can reach 90% [22].

Wind power is the fastest growing renewable energy generation method. Nowadays, there are large-scale wind power grid-connected operation, wind turbine generates electricity from wind energy conversion. The blades of the wind turbine

capture energy from the wind and convert it into rotational kinetic energy, and then through the mechanical drive system to transmit the mechanical energy to the generator, through the generator will be converted into the energy of the magnetic field, and ultimately converted into electrical energy. From the knowledge of aerodynamics of the wind turbine it can be concluded that the output power of the wind turbine is:

$$P_{WT} = \frac{1}{2}\rho \cdot \pi R_{WT}^2 \cdot v^3 \cdot C_P \tag{14}$$

where P_{WT} is wind turbine output power, ρ is the air density, R_{WT} is the radius of the wind turbine blades, πR_{WT}^2 is the swept area of the blades, v is the wind speed, C_P and is the wind energy utilization factor.

Photovoltaic power generation is a device that utilizes the photovoltaic effect unique to semiconductor p-n junctions and thus converts the energy of solar radiation into electrical energy. The characteristic of the output of a photovoltaic cell is:

$$I_{pv} = I_{ph} - I_{D0}\left(e^{\frac{q(U_{pv}+I_{pv}R_s)}{AKT}} - 1\right) - \frac{U_{pv}+I_{pv}R_s}{R_{sh}} \tag{15}$$

where, I_{pv} for the output current of the photovoltaic cell; I_{ph} for the current of the photogenerated current source; I_{D0} for the saturation current of the photovoltaic cell when there is no light; q is the electronic charge; R_s, R_{sh} respectively, for the series resistance of the photovoltaic cell and the side-drain resistance; K is Boltzmann's constant; A is the diode characteristic factor. The output power of the photovoltaic cell is related to the light intensity and voltage.

In order to maximize the use of renewable energy, in the analysis of this study we only consider the natural fluctuation of new energy output, which is regarded as a negative load and completely consumed, without considering its output regulation.

D. ENERGY STORAGE COST AND OPERATION MODEL

The lifetime of an energy storage system is related to its charging and discharging frequency, charging and discharging depth, and other factors. The energy storage cost modeling for global economic operation of the grid can be simplified appropriately. If the lifetime loss of the energy storage system is equalized to the charging and discharging loss per unit of electricity, the operating cost of the energy storage equipment F_{ES} can be expressed as follows:

$$F_{\mathrm{ES}} = \sum_t c_{es}(P_{es,c}^t + P_{es,d}^t)\Delta T \tag{16}$$

where, c_{es} is the loss cost corresponding to the unit charging quantity. $P_{es,c}^t$, $P_{es,d}^t$ is the charging and discharging power of the energy storage device in time period t, respectively. ΔT is the time step, 1h for day-ahead scheduling and 15min for intra-day scheduling. The energy storage device mainly contains the upper and lower charging and discharging power constraints, SOC constraints, and charging and discharging logic constraints.

Charging and discharging power upper and lower limit constraints:

When the energy storage is in charging or discharging state, the charging or discharging power shall not exceed the maximum power allowed by the system as shown in equation (17):

$$\begin{cases} 0 \le P_{es,c}^t \le P_{es,c}^{\max} u_{es,c}^t \\ 0 \le P_{es,d}^t \le P_{es,d}^{\max} u_{es,d}^t \end{cases} \tag{17}$$

where, $P_{es,c}^{\max}$ is the maximum charging power; $P_{es,d}^{\max}$ is the maximum discharging power; $u_{es,c}^t$ is the energy storage charging state quantity, $u_{es,d}^t$ is the energy storage discharging state quantity, the value is 0 or 1.

SOC constraint:

The real-time SOC of the energy storage is related to the charging and discharging power, efficiency, and the SOC of the previous time period, and the SOC can't exceed the upper and lower limits, as shown in equation (18):

$$\begin{cases} SOC_t = SOC_{t-1} + (\dfrac{P_{es,c}^t \eta_c}{E} - \dfrac{P_{es,d}^t}{E\eta_d})\Delta T \\ SOC_{\min} \le SOC_t \le SOC_{\max} \end{cases} \tag{18}$$

where, η_c is the charging efficiency, η_d is the discharging efficiency, E is the rated capacity of the energy storage, SOC_t is the SOC of the energy storage at time t, $SOC_{\min}$ is the lower limit of SOC, $SOC_{\max}$ is the upper limit of SOC.

Charging and discharging logic constraints:

Assuming that the energy storage is only in the charging or discharging state during a time period through scheduling operations, the charging and discharging logic constraint is shown in equation (19):

$$u_{es,c}^t + u_{es,d}^t \le 1 \tag{19}$$

III. CO-OPTIMIZATION MODEL FOR ISLAND DISTRIBUTION NETWORK SCHEDULING AND TOU

The cooperative optimization model of distribution network dispatching and tariff setting on the island takes micro fuel engines, energy storage, and active loads as control objects. In the day-ahead phase with 24h as the time scale, based on the short-term forecast results of Photovoltaic or wind power generation output and load and TOU-load phase response model, the economic operation of the distribution network is co-optimized with tariff-setting to determine the tariff and the basic operation mode of the distribution network for the next day. In the intra-day phase, the model predictive control algorithm is used to adjust the power of the control object in real time based on the photovoltaic or wind power generation and ultra-short-term load forecasting (USTLF) results and the IL corresponding model, using 4h as the time scale. For the USTLF, this paper draws on the methodology of [23]. The developed method is based on the integration of convolutional neural network (CNN) and long short-term memory (LSTM) network. The CNN module is used to capture the local trend of the load data pattern. It also flattened down the samples into a single one-dimensional vector, which is

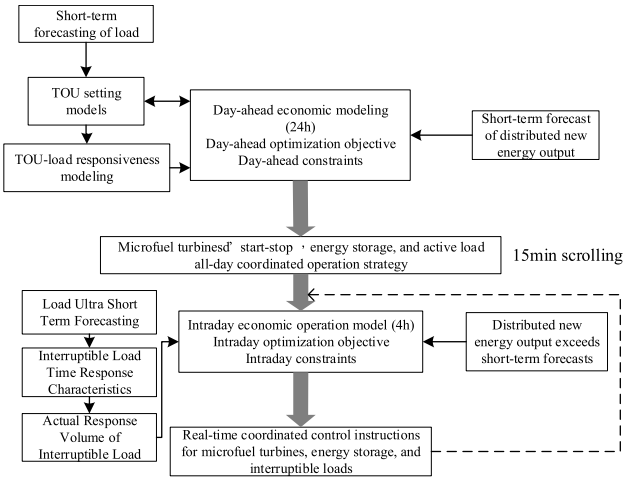

FIGURE 3. General architecture of co-optimization model for Island distribution network scheduling and TOU setting.

used as a single input time step to the LSTM layer. And study shows the strategy has higher precision and accuracy. The overall architecture of the active distribution network scheduling and tariff setting cooperative optimization model is shown in Figure 3:

Both the day-ahead and intraday scheduling phases, the distribution network scheduling mathematical model can be expressed as equation (20):

$$\max f(P, p, mo, u)$$
$$\text{s.}t \begin{cases} h(P, p, mo, u) = 0 \\ \underline{g} \le g(P, p, mo, u) \le \overline{g} \end{cases} \quad P, p \in R; mo, u \in \{0, 1\} \tag{20}$$

$f(P, p, mo, u)$ are the objective functions. $h(P, p, mo, u)$ and $g(P, p, mo, u)$ are the equation constraints and inequality constraints of the system, respectively. P, p, mo, u are the power, tariff, state transitions, and state variables, respectively.

A. A SYNERGISTIC OPTIMIZATION MODEL OF ECONOMIC OPERATION AND TOU FOR ISLAND DISTRIBUTION NETWORKS IN THE PAST FEW DAYS

The objective function of the synergistic optimization model of distribution network economic operation and tariff setting a few days ago is to maximize the total benefits for users and the grid:

$$f(P, p, mo, u) = f_1(P, p, mo, u) + f_2(p, L) \tag{21}$$
$$f_1(P, p, mo, u) = p \cdot L - C(P, p, mo, u) \tag{22}$$
$$f_2(p, L) = U(p, L) - p \cdot L \tag{23}$$

where, $f_1(P, p, mo, u)$ is the grid benefit, composed of tariff revenue $p \cdot L$ and power supply cost $C(P, p, mo, u)$. $f_2(p, L)$ is the user benefit, composed of user utility $U(p, L)$ and tariff revenue $p \cdot L$. p is the tariff and L is the load. The overall benefit depends on the user utility and grid operation cost, and is not directly related to the tariff p-L, but the change of tariff and load will indirectly affect the user utility and grid operation cost, and then affect the overall benefit.

In the case of electricity users, the measurement of user utility in existing TOU models usually uses a utility function. According to economic theory, the response behavior of electricity users usually takes the form of a quadratic function as follows [24]:

$$U(p, l) = \begin{cases} \omega l - \dfrac{\theta}{2} l^2, & 0 \le l \le \dfrac{\omega}{\theta} \\ \dfrac{\omega}{\theta}, & l > \dfrac{\omega}{\theta} \end{cases} \tag{24}$$

where, θ is a constant characterizing the sensitivity of the user's response to the tariff, usually taken as 0.5. l is the user's load demand. ω denotes the user's willingness to purchase electricity parameter, which has different values for different users at different times of the day. The value of user utility function can be obtained through market survey.

As far as the power system is concerned, the cost of power supply is mainly composed of generation cost F_t and distribution cost F_d, as shown in equation (25). Among them, the generation cost is the cost of purchasing electricity from the transmission grid, and in order to characterize the differences in generation cost under different operating powers, the generation cost adopts the typical synchronous unit generation cost function shown in equation (26). The main variable costs of power distribution depend on the operation mode of the distribution network, mainly including the operation cost of distributed micro fuel engine F_{MG}, the operation cost of energy storage F_{ES}, and the IL compensation cost F_L, as shown in equation (27):

$$C(P, p, sw, u) = F_t + F_d \tag{25}$$
$$F_t = a \cdot P_t^2 + b \cdot P_t + c \tag{26}$$
$$F_d = F_{MG} + F_{ES} + F_L \tag{27}$$

In the day-ahead optimization, the power balance constraints are mainly considered without taking into account network losses, etc., as shown in equation (28):

$$P_{MG,i}^t + P_{ES,i}^t + P_{NE,i}^t + \sum_l P_{l,i}^t = P_{L,i}^t \tag{28}$$

where, $P_{MG,i}^t$ is the micro fuel engine power at node i at time t, $P_{ES,i}^t$ is the energy storage power at node i at time t, $P_{NE,i}^t$ is the Photovoltaic or wind power generation power at node i at time t, and $P_{l,i}^t$ represents the power transmitted by the node line connected to node i at time t (with positive power flow to the node).

B. INTRADAY PHASE DISTRIBUTION NETWORK ECONOMIC OPERATION OPTIMIZATION MODEL

As the synergistic optimization of distribution network economic operation and tariff setting in the previous day's stage has initially determined the next day's tariff and the basic operation mode of the grid, the focus of intra-day economic operation is on real-time adjustment of power variables according to the ultra-short-term load forecasts and real-time

operation status of the grid, with the objective function of the lowest distribution network operation cost:

$$\min C_d = F_t + F_{MG} + F_{ES} + F_L \tag{29}$$

Since the model predictive control is used during the day with a time scale of 4h, the SOC state of the energy storage cannot take into account the whole day operation state and economy, so it is necessary to consider the storage SOC state in the constraints:

$$0.8 \cdot S^b_{\mathrm{ES}}(t) \le S^i_{\mathrm{ES}}(t) \le 1.2 \cdot S^b_{\mathrm{ES}}(t) \tag{30}$$

where $S^i_{\mathrm{ES}}(t)$ and $S^b_{\mathrm{ES}}(t)$ are the intraday and day-ahead energy storage SOC states, respectively.

In addition, since only power balance constraints are considered before the day, voltage and current overrun problems may occur during the intraday optimization process, so the necessary upper and lower current and voltage constraints need to be considered during the day. The real-time power balance of the grid will include the network loss power, which is modeled as follows:

$$V^2_{m,t} - V^2_{n,t} = 2(P_{mn,t} r_{mn} + Q_{mn,t} x_{mn}) + (r^2_{mn} + x^2_{mn}) \frac{P^2_{mn,t} + Q^2_{mn,t}}{V^2_{m,t}} \tag{31}$$

$$V^{\min}_{i,t} \le V_{i,t} \le V^{\max}_{i,t} \tag{32}$$

where m and n are the two ends of one line of the network. $V_{m,t}$, $V_{n,t}$ are the node voltage, $P_{mn,t}$, $Q_{mn,t}$ are the active and reactive power transmitted by the line. r_{mn}, x_{mn} and are the line resistance and reactance.

IV. MODEL SIMULATION

The integrated optimization model of TOU and grid operation developed in this paper is a mixed integer nonlinear programming problem (MINLP), so the open source software SCIP is used to solve it.

A. PARAMETERS OF THE ALGORITHMIC SYSTEM

In order to simulate the actual characteristics of the island power system, the IEEE 14-node distribution system is used as the basis for simulation analysis and related model settings. Node 2 is connected to a micro fuel engine with a power limit of 0.1 MW. Node 8 is connected to wind power and energy storage with a storage capacity of 1 MWh and a power limit of 0.3 MW. IL exists at node 14 with a capacity of 0.1 MW, $t_{i,0} = 2$h, $\lambda_0 = 1.6$, and a linear model is used for the time response characteristics of IL. The instantaneous response degree of IL of 0.5, and the response time is 1h. The baseline price of electricity is 0.6yuan/kWh. In order to characterize the changes in the cost of power generation in different time periods, the parameters of power purchase cost at the grid point b = 0, c = 0, and a takes the values of 400, 300, and 100 in the peak, flat, and valley time periods, respectively. Peak hours are 07:00-11:00 and 17:00-21:00, flat hours are 12:00-16:00 and 22:00-23:00, and valley hours are 00:00-6:00. Other detailed parameters of the distribution network, micro fuel engine and energy storage system are shown in Table 1 to 4. The number of users in each node is 10, and the example selects the typical TOU related data for simulation and analysis, and the parameters of the users' willingness to purchase electricity are shown in Table 5, and the price elasticity coefficients are shown in Table 6. The basic structure is shown in Figure 4. The model is in line with the characteristics of island distribution network such as user dispersion and few nodes, and has practical value.

TABLE 1. IEEE 14-node test system feeder parameters.

feeder starting point i	Feeder end point j	R_{ij}(per unit value)	X_{ij}(per unit value)
1	2	0.075	0.1
1	3	0.11	0.11
1	4	0.11	0.11
2	5	0.09	0.18
2	6	0.08	0.11
5	7	0.04	0.04
3	8	0.08	0.11
8	9	0.08	0.11
8	10	0.11	0.11
3	11	0.11	0.11
4	12	0.09	0.12
4	13	0.08	0.11
13	14	0.04	0.04

TABLE 2. Modified IEEE 14-node test system load rating parameters.

node number	P_l/kW	node number	P_l/kW
1	0	8	350
2	150	9	320
3	300	10	50
4	70	11	70
5	150	12	70
6	220	13	70
7	130	14	150

TABLE 3. Basic parameters of micro fuel engines.

type	value	type	value
price of natural gas (yuan/m^3)	3.45	heat loss coefficient	0.03
calorific value of natural gas (kWh m^3)	9.7	selling price of heat production (yuan/kWh)	0.1
generating efficiency	0.4	refrigeration selling price (yuan/kWh)	0.2
emission factor (yuan/MWh)	18.27	Startup and shutdown costs (yuan)	10
heating coefficient	1.2	power ceiling (MW)	0.1
cooling factor	0.95	lower power limit (MW)	0.02

B. SIMULATION STRATEGY

This paper proposes three strategies for comparative analysis to verify the effectiveness of the strategies proposed in this study:

TABLE 4. Basic parameters of energy storage.

type	value
charge/discharge losses (yuan/MWh)	30
charging efficiency	0.95
discharge efficiency	0.95
capacity (MWh)	1
power ceiling (MW)	0.3

TABLE 5. Parameters of users' willingness to purchase electricity ω.

time	Parameters of willingness to purchase electricity
valley hours	rand[5,7]
ground hours	rand[7,9]
peak hours	rand[9,10]

TABLE 6. Price elasticity coefficient.

time	valley	ground	peak
valley	-0.100	0.010	0.012
ground	0.010	-0.100	0.016
peak	0.012	0.016	-0.100

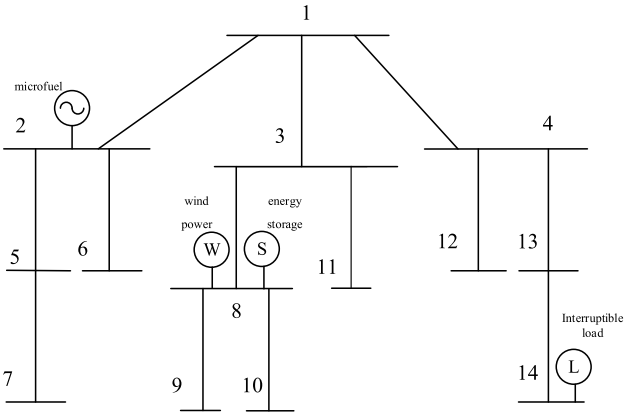

FIGURE 4. IEEE 14-node distribution system.

Strategy 1: Active load island distribution network scheduling based on TOU guidance proposed in this paper, with integrated optimization of TOU and economic operation;

Strategy 2: Island distribution network scheduling with constant tariff of 0.6 Yuan/kWh;

Strategy 3: Optimized scheduling of island distribution network without considering the mutual elasticity coefficient of loads, using the marginal cost method to determine TOU, and then the TOU as a known quantity.

Strategy 4: Based on the model proposed in this paper, the IL time-response characteristics are not considered, i.e., the IL is considered to be instantly removed as per the predetermined instruction during the optimization process.

C. STRATEGY 1 PRE-DAY AND INTRA-DAY DISPATCH RESULTS ANALYSIS

By solving the strategy 1 model, the TOU for each hour of the previous day can be obtained, as well as the load response curve under the action of this TOU, as shown in Figure 5.

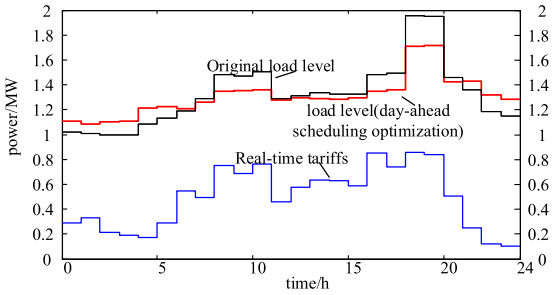

FIGURE 5. Day-ahead TOU and load changes.

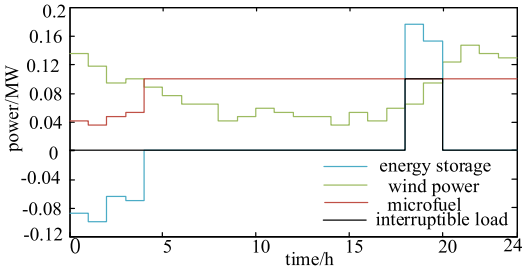

(a) energy storage, wind power, micro fuel, interruptible load curve

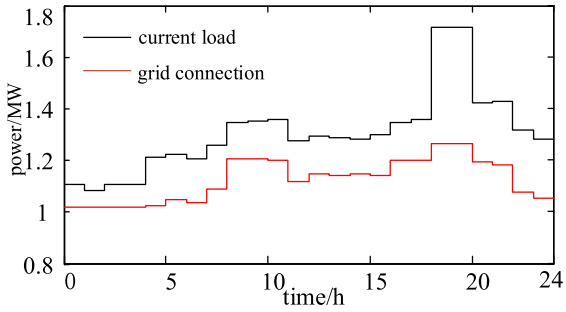

(b) current load, grid connection curve

FIGURE 6. Power curve of each unit in the first day stage.

It can be seen that under the effect of TOU, the peak-to-valley difference of load is obviously reduced, which reduces the regulation pressure of the grid. The TOU strategy proposed in Strategy 1 basically presents the feature that the higher the load, the higher the tariff, and its pricing is not only related to the load level at this time, but also affected by the tariffs of other times of the day in the distribution network. Strategy 1 achieves the synergistic optimization of market tariff and grid economic operation.

Figure 6 and 7 show the power curves of each unit of the active distribution network and the storage operation status in the optimization phase a few days ago. From the figures, it can be seen that when the load is high, without reducing the operating cost, the micro fuel burner will be put into operation and IL removed. When the load is low, the micro fuel engine does not run or runs at low power, while the IL is put into operation. Energy storage shaves peaks and fills valleys by charging and discharging to improve the economy of the whole network operation.

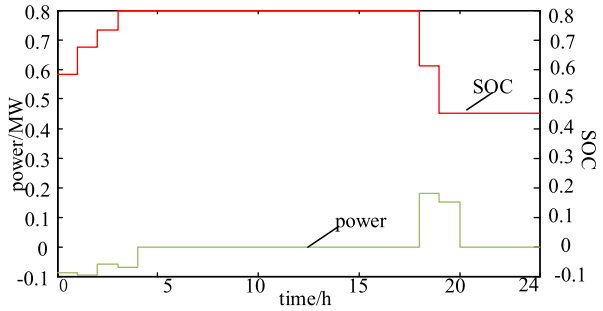

FIGURE 7. Day-ahead energy storage operation status.

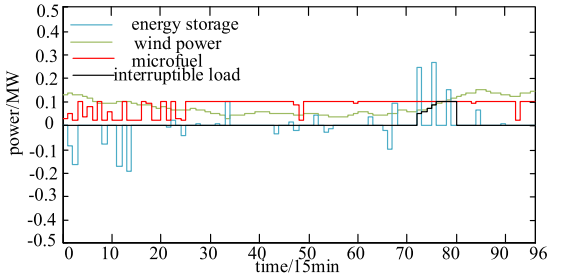

(a) energy storage, wind power, micro fuel, interruptible load curve

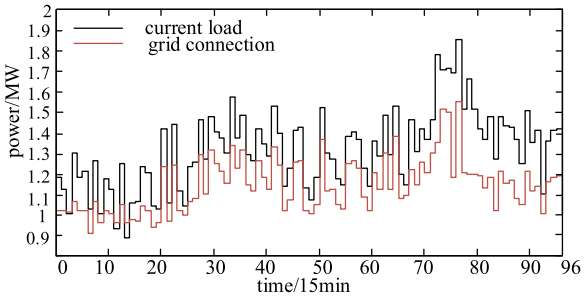

(b) current load, grid connection curve

FIGURE 8. Power curves of the units in the intraday phase.

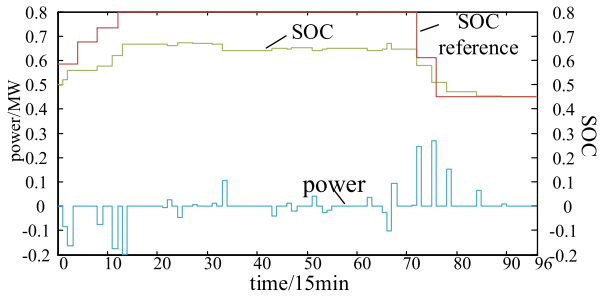

FIGURE 9. Intraday phase energy storage system power and SOC states.

Based on the above results of the day-ahead optimization and control, the example data are kept unchanged, and the simulation analysis of the intra-day rolling optimization is carried out. The results of the all-day rolling optimization are shown in Figure 8. The storage charging and discharging power and SOC states are shown in Figure 9, where the SOC reference value is the result of the day-ahead stage optimization.

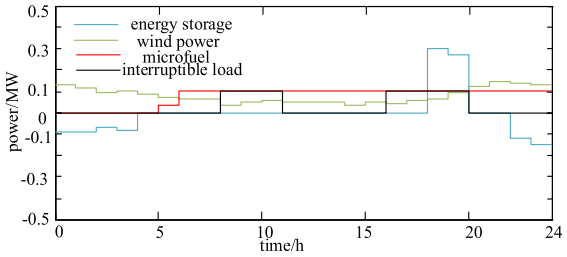

(a) energy storage, wind power, micro fuel, interruptible load curve

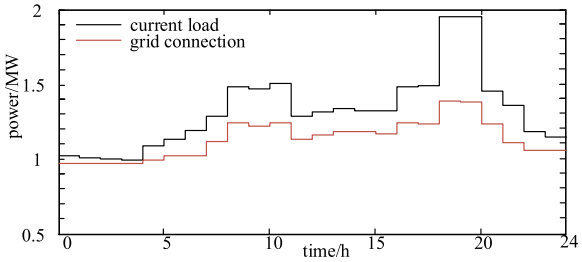

(b) current load, grid connection curve

FIGURE 10. Power curves of each unit in the day-ahead stage when strategy 2 is adopted.

As can be seen in Figure 8, in general, the overall trend of the intraday rolling optimization results is similar to that of the day-ahead optimization results, but the intraday optimization results are more fine-grained and reflect the real-time load fluctuations. In addition, the intraday stage optimization model introduces the energy storage system SOC constraint equation (22) based on the day-ahead optimization results. From Figure 9, it can be seen that the intraday storage charging and discharging depth is smaller than that of the previous day, which is due to the smaller load peak-valley difference in the intraday optimization time scale (4h), and the energy storage tends not to be charged or discharged. Taking 0:00-4:00 as an example, the load peak-valley difference is very small, and if the intraday SOC optimization is not considered, the energy storage will not be charged, resulting in the failure to provide sufficient power during the 18:00-20:00 time period. In contrast, by introducing the coordination of SOC constraints based on the day-ahead scheduling results, the energy storage has to be charged to increase the SOC to 0.65, giving it more sufficient power to meet the peak-load demand during 18:00-20:00.

D. COMPARATIVE ANALYSIS OF STRATEGY 1 AND STRATEGY 2 (TOU VS. CONSTANT TARIFF)

The results of the day-ahead stage optimization when strategy 2 is used are shown in Figure 10. The storage charging and discharging power and SOC states are shown in Figure 11. A comparison of the cost and benefit results for each part of the distribution network in Strategy 1 and Strategy 2 is shown in Table 7.

In strategy 1, the utility function of the user is relatively low, but after considering the daily electricity cost, the user benefit is increased by 2,629 yuan compared with strategy 2.

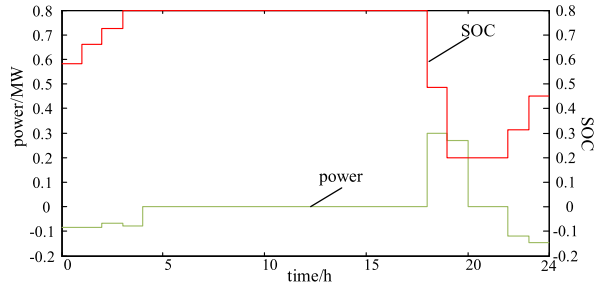

FIGURE 11. Day-ahead stage energy storage operation state when strategy 2 is adopted.

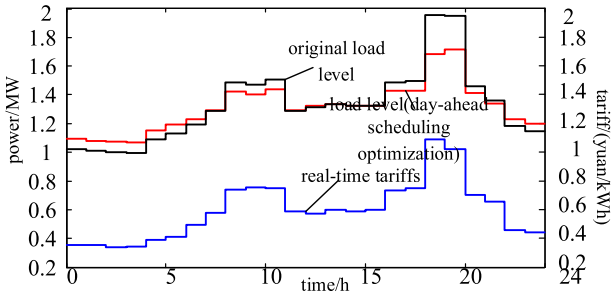

FIGURE 12. TOU and load changes in the day-ahead phase when strategy 3 is adopted.

TABLE 7. Comparison of costs and benefits between strategy 1 and strategy 2.

type of cost/benefit	strategy 1 (yuan)	strategy 2 (yuan)
costs of purchasing power at grid connection	8989	9213
energy storage operating costs	249	294
Micro fuel engine operating costs	1348	1134
IL calling costs	144	504
grid operating costs	10730	11145
user utility function	17932	18308
overall benefits	7202	7163

Meanwhile, for the grid, since Strategy 1 can guide the user's electricity consumption through TOUs to adapt to scheduling, the grid operation cost is lower, but under the influence of the market, the grid tariff benefit is reduced, and the accounted grid benefit is reduced by 2,590 yuan. However, synthesizing the interests of both users and the grid, the reduction of user utility is lower than the reduction of grid costs. At the same time, for the grid, but after the adoption of strategy 1, while shaving peaks and filling valleys of loads, it will produce positive externalities, reduce system expansion costs, reduce system standby costs, and further reduce the cost of the grid and so on. Therefore, from the final overall comprehensive benefits, strategy 1 is higher than strategy 2.

E. COMPARATIVE ANALYSIS OF THE RESULTS OF STRATEGY 1 AND STRATEGY 3 (TOU AND DISTRIBUTION NETWORK OPERATION INTEGRATION OPTIMIZATION)

To further illustrate the superiority of the integrated optimization of TOUs and economic operation, a comparison strategy (Strategy 3) is designed, i.e., TOU and grid operation are optimized in steps:

1. Pricing stage: the mutual elasticity coefficient of load is not considered, i.e., the price of electricity in each time period only depends on the cost (generation cost, network loss, etc.) and revenue (combined revenue of the grid and the customer) in that time cross-section, and does not take into account the scheduling of energy storage and IL.

2. operation phase: the TOU determined in the pricing phase is used as a known quantity, and the model in this chapter is used to optimize the dispatch of the distribution network.

The difference between Strategy 1 and Strategy 3 is that; Strategy 1 uses the coordinated optimization of real-time prices and grid economic dispatch; while Strategy 3 only considers the self-elasticity coefficients of the loads in each time period, and optimizes the distribution network based on the results of market prices optimization.

After adopting strategy 3, the TOU obtained from the optimization in the previous day stage are shown in Figure 12 with the corresponding load changes, and the distribution network operating power curve is shown in Figure 13. Comparison of costs and benefits of each part of the distribution network in Strategy 1 and Strategy 3 is shown in Table 8.

For strategy 3, in the pricing stage, the cost of grid operation only considers the cost of generation, i.e., the cost of purchasing electricity at the grid connection point as well as the cost of running the micro fuel engine, and the optimization process will minimize the two costs and increase the user's utility, which is shown in Table 8, where the cost of purchasing electricity at the grid connection point and the cost of running the micro fuel engine have been reduced by 103 yuan and 148 yuan, respectively, and the user's utility has been increased by 92 yuan. Compared with Strategy 1, Strategy 3 increases the benefit by a total of 343 yuan in the above three indicators. Therefore, if only TOU pricing is considered, since Strategy 3 does not take into account the constraints of scheduling, its TOU setting has more optimization space, making the results of Strategy 3 better than the strategies in this chapter. However, when carrying out the distribution network economic operation optimization, since the tariffs formulated using Strategy 3 do not take into account its impact on the distribution network operation, the load profiles obtained from its guidance cannot be optimally matched with the operation scheduling. As can be seen from Figure 13, its storage charging and discharging amplitude is larger and the IL call time is longer, resulting in higher costs of 3 yuan and 360 yuan, respectively. Taking into account the aforementioned increase in dispatch costs, the reduced costs and increased benefits of Strategy 3 in the pricing stage are completely offset, which ultimately makes the overall benefits of Strategy 3 lower than those of Strategy 1 instead.

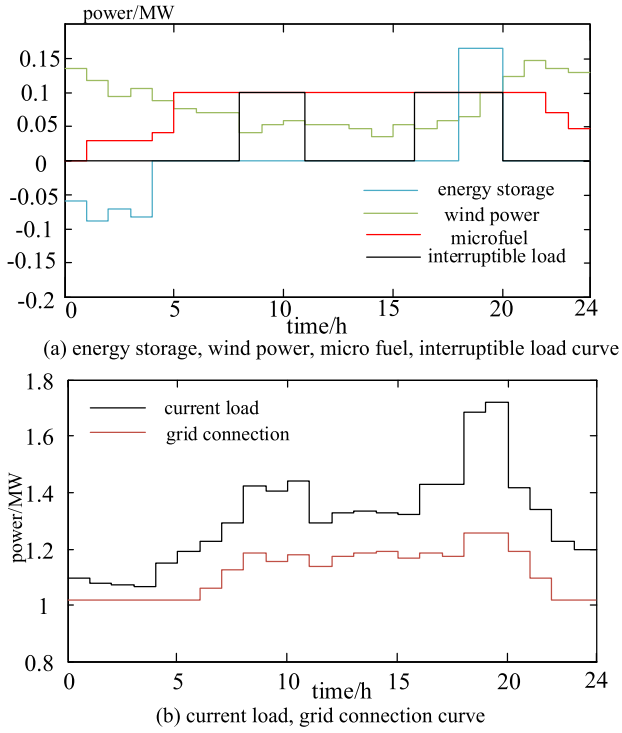

FIGURE 13. Power curves of each unit in the day-ahead stage when strategy 3 is adopted.

TABLE 8. Comparison of costs and benefits between strategy 1 and strategy 3.

type of cost/benefit	strategy 1 (yuan)	strategy 3 (yuan)
costs of purchasing power at grid connection	9189	9086
energy storage operating costs	49	52
Micro fuel engine operating costs	1348	1200
IL calling costs	144	504
grid operating costs	10730	10842
user utility function	17932	18024
overall benefits	7202	7182

F. COMPARATIVE ANALYSIS OF THE RESULTS OF STRATEGY 1 VERSUS STRATEGY 4 (WITH OR WITHOUT CONSIDERATION OF IL TIME RESPONSE CHARACTERISTICS)

The strategy in this paper considers the IL time response characteristics in the optimization process, i.e., when the actual load is delayed to be removed, the optimization strategy is adjusted for the delayed case to obtain the most economical operation in the delayed case. To illustrate the superiority of this consideration, strategy 4 is set up for comparison. Combining the day-ahead optimization results of Strategy 1, the grid removes 0.1 MW of IL at 18:00, and since the instantaneous response amount is 0.5 and the response time is 1 h, the IL is actually removed by 0.05 MW at 18:00 and the remaining 0.05 MW at 19:00, but Strategy 4 is optimized on the basis that the IL is removed in full at 18:00.

Considering that the intraday optimization time scale is 4h, we only focus on the simulation near the 18:00-20:00 time

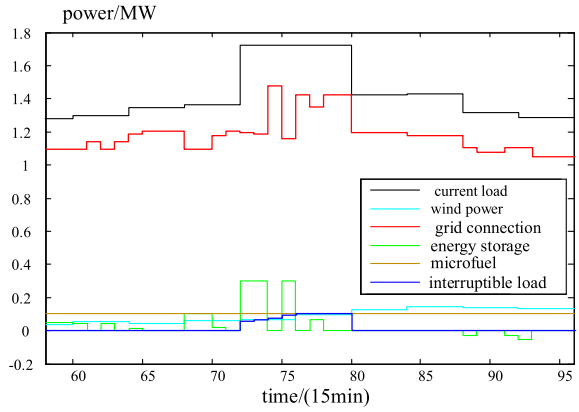

FIGURE 14. Power curves of the units in the intraday phase when strategy 1 is adopted.

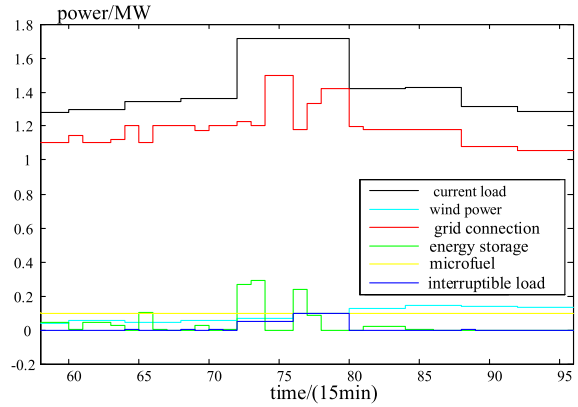

FIGURE 15. Power curves of the units in the intraday phase when strategy 4 is adopted.

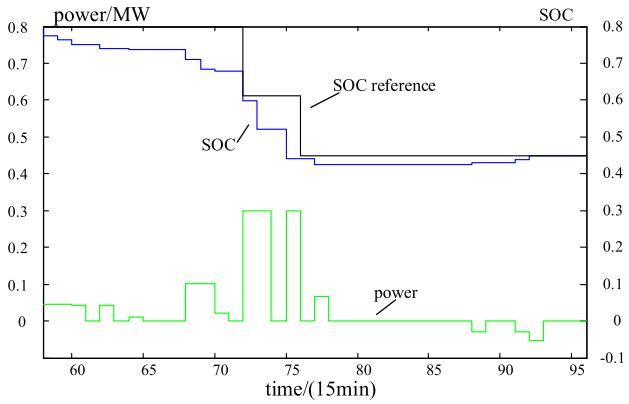

FIGURE 16. Intraday phase energy storage power and SOC curve when strategy 1 is adopted.

period, and set the initial SOC state of the energy storage to 0.8. The optimization calculations are carried out by using strategy 1 and strategy 4, respectively, and the simulation results are as follows:

For strategy 4, since the actual load value (current load value minus IL removal) during 18:00-19:00 is 0.05 MW higher than the load identified by the optimization process, this excess power can only be passively provided by the

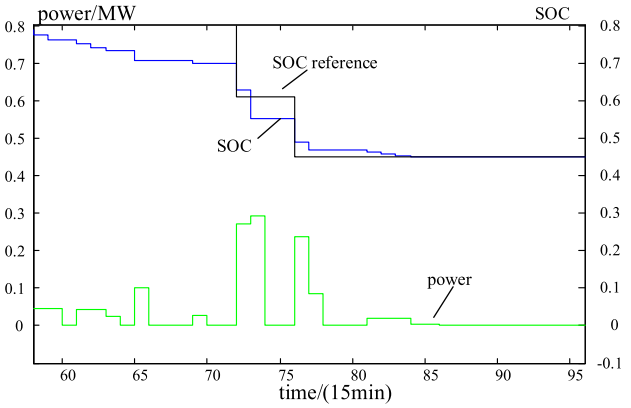

FIGURE 17. Intraday phase energy storage power and SOC curve when strategy 4 is adopted.

TABLE 9. Comparison of costs and benefits between strategy 1 and strategy 4.

type of cost/benefit	strategy 1 (yuan)	strategy 4 (yuan)
costs of purchasing power at grid connection	4197.4	4209.7
energy storage operating costs	121.5	118.0
Micro fuel engine operating costs	597.8	597.7
IL calling costs	144	144
grid operating costs	5060.7	5069.4

grid-connected point, resulting in an increase in the cost of power purchased by the grid-connected point. For strategy 1, because 0.05MW less IL is removed at 18:00, the actual load value from 18:00 to 19:00 is 0.05MW higher than that from 19:00 to 20:00, and the energy storage is concentrated to be discharged in the period of 18:00 to 19:00, and the magnitude of discharge is larger than in strategy 4, and the cost of storage operation is higher than that in strategy 4. However, the magnitude of the increase is significantly smaller than the increase in cost of grid-connected points in strategy 4 relative to strategy 1, which indicates that the cost of power purchased by the grid-connected points in strategy 1 is increased. However, the increase in storage operating costs is significantly smaller than the increase in grid connection point costs for Strategy 4 relative to Strategy 1, indicating that strategy 1 can achieve economic optimization by reasonably adjusting the charging and discharging behavior of energy storage. In summary, the strategy in this paper achieves more refined control, and the optimization results are better than strategy 4.

V. CONCLUSION

We have developed a coordinated optimization model for island distribution network scheduling and TOU setting by synergizing TOU with grid economic operation optimization and taking into account the time response characteristics of IL. Considering the characteristics of the island distribution network, the following conclusions are obtained based on the theoretical analysis and the results of the arithmetic test using the IEEE14 node system as an example:

(1) Compared with the existing constant tariff mechanism, the TOU mechanism improves the utility of the customer side by 2,629 yuan and reduces the grid revenue by 2,590 yuan, and the reduced grid revenue is smaller than the increased customer utility, so the TOU mechanism is able to improve the overall revenue of the supply and demand sides.

(2) By comparing the two strategies of TOU with or without considering grid dispatch, it is concluded that the strategy that only considers the TOU mechanism has a total economic benefit of 343 yuan on the side of user utility and generation cost, but the cost of energy storage and the cost of IL call is increased by a total of 363 yuan. Therefore, the co-optimization of TOU pricing with grid dispatch operation can obtain better economic benefits.

(3) By comparing whether the time response of IL is considered in the co-optimization strategy, it is concluded that when the time response of IL is considered, the cost of energy storage operation increases but the cost of power purchase at the grid connection point decreases. It also proves the necessity of considering the IL time response by achieving a more fine-grained control.

In summary, the synergistic optimization of TOU and grid scheduling considering IL time characteristics improves the economic efficiency of island distribution network operation.

However, the load price elasticity coefficient method and the user utility function model used in this paper are simple, and the established user response model is only based on theoretical analysis, which will differ from the actual situation. Therefore, how to properly consider the adverse effects of prediction errors on scheduling models and overcome them will be the focus of future research.

REFERENCES

[1] D. Groppi, F. Feijoo, A. Pfeifer, D. A. Garcia, and N. Duic, "Analyzing the impact of demand response and reserves in islands energy planning," *Energy*, vol. 278, Sep. 2023, Art. no. 127716.

[2] Z. Sang, J. Huang, J. He, R. Fang, J. Yan, and H. Lei, "The integrated energy system with multiple resources integration in future distribution network of pelagic clustering islands," *J. Coastal Res.*, vol. 108, pp. 42–47, Aug. 2020.

[3] K. H. Mohd Azmi, N. A. Mohamed Radzi, N. A. Azhar, F. S. Samidi, I. Thaqifah Zulkifli, and A. M. Zainal, "Active electric distribution network: Applications, challenges, and opportunities," *IEEE Access*, vol. 10, pp. 134655–134689, 2022.

[4] G. Wang, X. Lei, H. Wu, K. Sun, L. Wang, Y. Ding, and C. Wang, "A comprehensive network restoration model for active distribution network considering forecast uncertainty," *IEEE Access*, vol. 9, pp. 130997–131005, 2021.

[5] M. E. Honarmand, V. Hosseinnezhad, B. Hayes, M. Shafie-Khah, and P. Siano, "An overview of demand response: From its origins to the smart energy community," *IEEE Access*, vol. 9, pp. 96851–96876, 2021.

[6] L. Wen, K. Zhou, W. Feng, and S. Yang, "Demand side management in smart grid: A dynamic-price-based demand response model," *IEEE Trans. Eng. Manag.*, vol. 71, no. 1, pp. 1–30, Jan. 2022.

[7] N. Wu, H. Wang, L. Yin, X. Yuan, and X. Leng, "Application conditions of bounded rationality and a microgrid energy management control strategy combining real-time power price and demand-side response," *IEEE Access*, vol. 8, pp. 227327–227339, 2020.

[8] M. K. Mishra and S. K. Parida, "A game theoretic approach for demand-side management using real-time variable peak pricing considering distributed energy resources," *IEEE Syst. J.*, vol. 16, no. 1, pp. 144–154, Mar. 2022.

[9] Z. Guo, W. Xu, Y. Yan, and M. Sun, "How to realize the power demand side actively matching the supply side?—A virtual real-time electricity prices optimization model based on credit mechanism," *Appl. Energy*, vol. 343, Aug. 2023, Art. no. 121223.
[10] C. Wang, M. Ni, Y. Shi, L. Zhang, W. Li, and X. Li, "Optimizing power market clearing with segmented electricity prices: A bilevel model," *Sustainability*, vol. 15, no. 18, p. 13575, Sep. 2023.
[11] K. Aurangzeb, S. Aslam, S. M. Mohsin, and M. Alhussein, "A fair pricing mechanism in smart grids for low energy consumption users," *IEEE Access*, vol. 9, pp. 22035–22044, 2021.
[12] M. Heidarpanah, F. Hooshyaripor, and M. Fazeli, "Daily electricity price forecasting using artificial intelligence models in the Iranian electricity market," *Energy*, vol. 263, Jan. 2023, Art. no. 126011.
[13] W. Li and D. M. Becker, "Day-ahead electricity price prediction applying hybrid models of LSTM-based deep learning methods and feature selection algorithms under consideration of market coupling," *Energy*, vol. 237, Dec. 2021, Art. no. 121543.
[14] G. Chen, X. Zhang, C. Wang, Y. Zhang, and S. Hao, "Research on flexible control strategy of controllable large industrial loads based on multi-source data fusion of Internet of Things," *IEEE Access*, vol. 9, pp. 117358–117377, 2021.
[15] H. Yang, S. Zhang, J. Zeng, S. Tang, and S. Xiong, "Future of sustainable renewable-based energy systems in smart city industry: Interruptible load scheduling perspective," *Sol. Energy*, vol. 263, Oct. 2023, Art. no. 111866.
[16] M. U. Saleem, M. R. Usman, M. A. Usman, and C. Politis, "Design, deployment and performance evaluation of an IoT based smart energy management system for demand side management in smart grid," *IEEE Access*, vol. 10, pp. 15261–15278, 2022.
[17] F. Luo, W. Kong, G. Ranzi, and Z. Y. Dong, "Optimal home energy management system with demand charge tariff and appliance operational dependencies," *IEEE Trans. Smart Grid*, vol. 11, no. 1, pp. 4–14, Jan. 2020.
[18] J. Wang, H. Ge, Z. Pan, H. Zhao, B. Wang, and T. Xia, "Multi-type reserve collaborative optimization for gas-power system constrained unit commitment to enhance operational flexibility," *Electronics*, vol. 12, no. 19, p. 4029, Sep. 2023.
[19] G. Ma, Z. Cai, P. Xie, P. Liu, S. Xiang, Y. Sun, C. Guo, and G. Dai, "A bi-level capacity optimization of an isolated microgrid with load demand management considering load and renewable generation uncertainties," *IEEE Access*, vol. 7, pp. 83074–83087, 2019.
[20] R. Chandra, S. Banerjee, K. K. Radhakrishnan, and S. K. Panda, "Transactive energy market framework for decentralized coordination of demand side management within a cluster of buildings," *IEEE Trans. Ind. Appl.*, vol. 57, no. 4, pp. 3385–3395, Jul. 2021.
[21] P. Roy, J. He, T. Zhao, and Y. V. Singh, "Recent advances of wind-solar hybrid renewable energy systems for power generation: A review," *IEEE Open J. Ind. Electron. Soc.*, vol. 3, pp. 81–104, 2022.
[22] S. V. Medina and U. P. Ajenjo, "Performance improvement of artificial neural network model in short-term forecasting of wind farm power output," *J. Modern Power Syst. Clean Energy*, vol. 8, no. 3, pp. 484–490, May 2020.
[23] S. H. Rafi, Nahid-Al-Masood, S. R. Deeba, and E. Hossain, "A short-term load forecasting method using integrated CNN and LSTM network," *IEEE Access*, vol. 9, pp. 32436–32448, 2021.
[24] D. Liu, Y. Sun, B. Li, X. Xiangying, and L. Yudong, "Differentiated incentive strategy for demand response in electric market considering the difference in user response flexibility," *IEEE Access*, vol. 8, pp. 17080–17092, 2020.

WEIJIE HE received the B.S. degree in electrical engineering from the Huazhong University of Science and Technology, Wuhan, China, in 2023, where he is currently pursuing the master's degree in electrical engineering. His research interest includes optimal control of power systems.

LANXUAN GUO received the B.S. degree in electrical engineering from Shandong University, Jinan, China, in 2023. She is currently pursuing the Ph.D. degree in electrical engineering with the Huazhong University of Science and Technology, Wuhan, China. Her main research interest includes optimal control of power systems.

WENHAO YANG received the B.S. degree in electrical engineering from the Huazhong University of Science and Technology, Wuhan, China, in 2023, where he is currently pursuing the master's degree in electrical engineering. His main research interest includes optimal control of power systems.

XIANGNING LIN (Senior Member, IEEE) was born in Guangxi, China, in 1970. He received the M.S. and Ph.D. degrees in electrical engineering from the Huazhong University of Science and Technology (HUST). He is currently a Full Professor with HUST. His research interests include microgrid scheduling, modern signal processing, and power system protective relay.

FANRONG WEI received the Ph.D. degree in electrical engineering from the Huazhong University of Science and Technology (HUST). His research interests include optimal power system/microgrid scheduling and protective relay.

SAMIR M. DAWOUD received the B.Sc. and M.Sc. degrees in electrical power and machines engineering from Tanta University, Egypt, and the Ph.D. degree in electrical engineering from the Huazhong University of Science and Technology, China, in 2017. He is currently an Associate Professor with the Electrical Engineering Department, Tanta University. His current research interests include renewable energy, power system planning, microgrid planning optimization, and power system reliability.